Journal Name

ARTICLE

Predicting the Reducing Power of Organic Super Electron Donors†

Greg M. Anderson,[a] Iain Cameron,[a] John A. Murphy,[a]* Tell Tuttle[a]*

Received 00th January 20xx,
Accepted 00th January 20xx

DOI: 10.1039/x0xx00000x

www.rsc.org/

The utilization of computational methods to predict reactivity is an increasingly useful tool for chemists to save time and materials by screening compounds for desirable reactivity prior to testing in the laboratory. In the field of electron transfer reactions, screening can be performed through the application of Marcus Hush theory to calculate the activation free energy of any potential reaction. This work describes the most accurate and efficient approach for modelling the electron transfer process. In particular, the importance of using an electron transfer complex to model these reactions rather than considering donor and acceptor molecules as separate entities is highlighted. The use of the complex model is found to produce more accurate calculation of the electron transfer energy when the donor and acceptor spin densities are adequately localised.

Introduction

Electron transfer reactions play a central role in a variety of different transformations, ranging from biological processes (e.g. photosynthesis[1] and metabolism[2]) to a number of laboratory-based chemistries such as the Birch reduction.[3] Predominant within the recent literature are areas such as the application of photovoltaics,[4] photoredox catalysis[5] and, more recently, transition metal-free coupling reactions.[6] The importance of these reactions across a range of fields has led to a significant drive to move chemistry in a direction where costly and potentially toxic transition metal-based reagents can be substituted for cheaper, more benign organic-based reagents. For example, König has demonstrated the ability of organic dyes such as eosin Y[7] and perylene diimides[8] to act as electron donors upon photoactivation. These activated molecules can then reduce arenediazonium salts[7] and aryl halides[8] respectively to the corresponding aryl radicals, which can then undergo a coupling reaction to afford various biaryl products.

Over recent years, a number of research groups have published results demonstrating the ability of a wide range of organic molecules (Scheme 1), in the presence of a strong base (most commonly potassium *tert*-butoxide), to promote the formation of biaryl products from haloarenes in the absence of any transition metal catalyst.[9-18] This research has stemmed from the initial findings of Itami *et al.*,[19] who demonstrated that aryl iodides could be coupled to heteroarenes such as pyridine (used as the reaction solvent) in the presence of potassium *tert*-butoxide. The proposal of Studer and Curran,[20] that these reactions proceed by the base-promoted homolytic aromatic substitution (BHAS) cycle is widely accepted (Scheme 2).

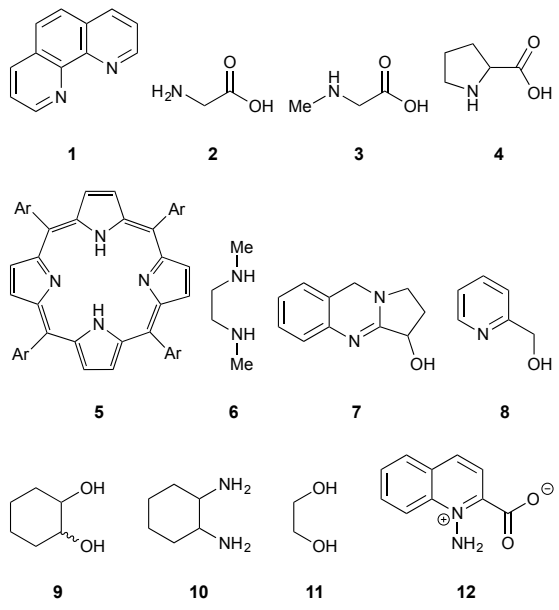

Scheme 1. Examples of organic molecules shown to promote biaryl coupling reactions in the presence of potassium tert-butoxide.

[a] *WestCHEM, Department of Pure and Applied Chemistry, University of Strathclyde, 295 Cathedral Street, Glasgow, G1 1XL, United Kingdom.*
**corresponding author: john.murphy@strath.ac.uk*
**corresponding author: tell.tuttle@strath.ac.uk*

†Electronic Supplementary Information (ESI) available: [Optimised reaction coordinates and geometries, Model 2 HOMO, LUMO and Spin Density graphics]. See DOI: 10.1039/x0xx00000x

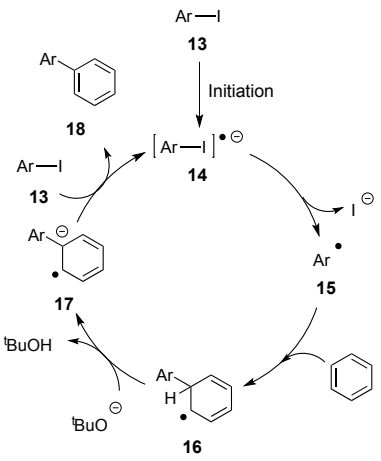

Scheme 2. A Summary of the BHAS reaction cycle.

Our research group has a strong interest in the application of organic reagents in electron transfer reactions, and has developed a number of neutral organic super electron donors (SED's) that are capable of performing a variety of chemical reductions.[21] We have recently proposed the structures for the active electron transfer reagents in a number of these metal-free coupling reactions, based on experimental observations.[22, 23] For example, donor **19** and/or it's corresponding monoanion has been shown to form from **1** under the reaction conditions employed.[22] This was demonstrated by the isolation of the neutral oxidised form of **19** upon quenching with iodine. Traditionally, neutral SED's such as **21** are formed prior to use by reaction of the corresponding disalt, in this instance **20**, with sodium hydride.[24] However, we have also demonstrated that the disalt **20** can be used directly under the conditions typically used for these metal-free coupling reactions to afford the desired product, indicating the ability of potassium *tert*-butoxide to generate the organic SED **21** *in situ* (Scheme 3).[22]

In order to move this chemistry forward, it is desirable to design and develop new, more powerful electron donors that allow the electron transfer to occur at lower reaction temperatures and widen the current substrate scope of aryl iodides and, in some cases, aryl bromides to a broader selection of aromatic substrates. The ability to mediate these transformations at lower reaction temperatures with aryl chlorides would allow for greater competition with transition metal-based reaction conditions. Encouraging steps towards this level of reactivity have already been demonstrated by Dyker *et al.*,[25] who have recently developed a neutral tetra(iminophospherano)-substituted bispyridinylidene donor with a redox potential exceeding that of neutral organic donors previously developed within our group. This new donor was capable of reactivities previously only accessible using our donors under photoactivated reaction conditions. An attractive means of aiding the design process is the application of computational methods to screen potential electron donors, and their precursors, to determine whether or not they are viable candidates.

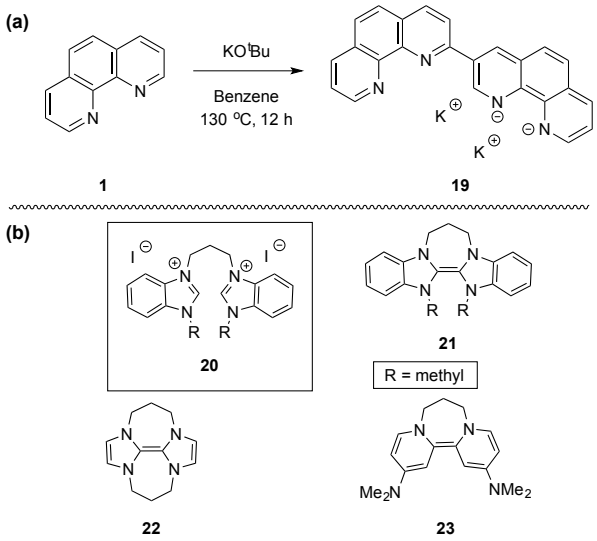

Scheme 3. Proposed SED formed from reaction of 1,10-phenanthroline **1** with potassium tert-butoxide (a) and examples of a disalt precursor and neutral SED's used within our research group (b).

The Marcus Theory for electron transfer is commonly applied to the study of a number of different chemical systems, ranging from the work of Kochi *et al.* on the study of ion pair intermolecular electron transfers[26-28] to the study of lithium-air batteries by Banerjee and co-workers.[29] Similarly, this theory has also been applied within a biochemical context and Blumberger has recently published an excellent review article in which QM/MM has been applied to calculate the energetics for the electron transfer in a modified cytochrome c system. [30] Within our own lab, we have previously used computational methods to investigate the relative abilities of neutral SED's to reduce aryl halides.[31] In using related methods within this work to investigate the potential ability of candidate organic electron donors, our aim is to ensure that the assumptions made in these calculations are valid. Notable differences between the previous work and the present work are the choice of solvent (previously *N*,*N*-dimethylformamide was used; present reactions are performed in benzene) and the charge state of the electron donors (the present proposed electron donors are anionic or dianionic in nature). One crucial aspect of these differences is the treatment of the donor and acceptor molecules as a single complex. The use of electron transfer complexes versus Nelsen's four-point method[32] may play a more significant role when considering non-neutral donors and acceptors. Therefore, it is necessary to determine which model most accurately predicts reaction energetics by comparison with experimental observation, as summarised in Figure 1 below. In addition to this, the formation of the proposed donors by reaction with potassium *tert*-butoxide is also investigated to determine how effectively the potential donors can be formed under standard reaction conditions. The use of donor-acceptor complexes in Model 2 does not consider the effects of extrinsic factors discussed by Himmel,[33] such as solvent reorganisation. However, given the larger solvent exclusion afforded by considering the full complex and the use of a continuum solvent approach, the effect of this approximation should be minimised.

Journal Name

ARTICLE

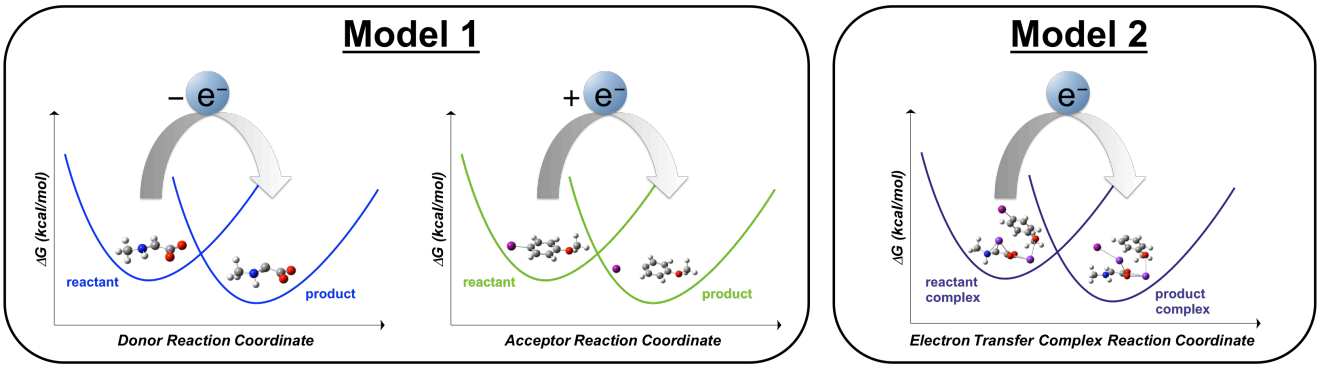

Figure 1. Graphical summary of the reaction models investigated in this study.

Theoretical Details

The study of electron transfer reactions using computational methods is possible largely due to the work of Rudolph Marcus, who formulated his theory for the calculation of electron transfer reaction activation free energies in the 1960's.[34] Calculation of these barriers, ΔG^*, is based on two factors; the total reorganisation energy of the system λ and the relative free energy ΔG_{rel} (Eq. 1)

$$\Delta G^* = \frac{\lambda}{4}\left(1 + \frac{\Delta G_{rel}}{\lambda}\right)^2 \qquad \text{(Eq. 1)}$$

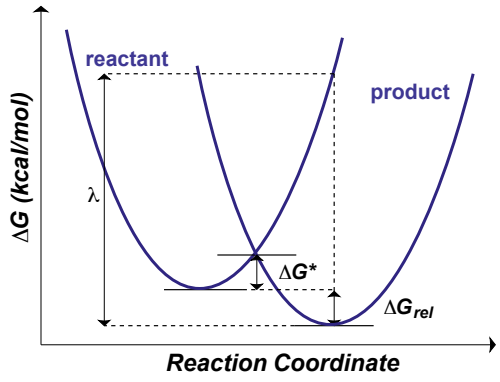

Figure 2. Energy diagram for the calculation of electron transfer reactions by Marcus Theory.

The potential energy surface of two half reactions can be considered as separate parabolas, and thus Marcus Hush theory can be illustrated as per Figure 2. The intersection of these parabolas represents the activation free energy ΔG^*, while the energy difference between the two minima represents the relative free energy ΔG_{rel}. The reorganisation energy λ is interpreted as the vertical energy difference between the minimum of the product curve and the point where the reactant curve overlaps with this on the potential energy surface.

The total reorganisation energy of the system λ is comprised of the internal reorganisation λ_i (electron donor and acceptor molecules) and the external reorganisation energy λ_o (i.e., the reorganisation of the solvent in response to the electron transfer). Research published by Kochi[26-28] and Banerjee[29] has demonstrated that in calculating the overall reorganisation energy, the internal reorganisation energy has a more significant influence on the total reorganisation energy relative to the external reorganisation energy. The opposite of this was observed in Blumberger's study on biological systems.[30] However, the current systems under study exist in a non-strongly coordinated medium and as such are more akin to the systems studied by Kochi[26-28] and Banerjee.[29] Therefore, with this in mind, (Eq. 1) can be reduced to the following (Eq. 2), accounting only for the internal reorganisation energy contribution:

$$\Delta G^* = \frac{\lambda_i}{4}\left(1 + \frac{\Delta G_{rel}}{\lambda_i}\right)^2 \qquad \text{(Eq. 2)}$$

The internal reorganisation energy is calculated as follows (Eq. 3):

$$\lambda_i = \frac{\lambda_i(D) + \lambda_i(A)}{2} \qquad \text{(Eq. 3)}$$

where $\lambda_i(D)$ represents the internal reorganisation energy for the electron donor and $\lambda_i(A)$ represents the internal reorganisation energy for the electron acceptor. The internal

reorganisation energy for a given species is typically calculated using Nelsen's four-point method,[32] which for the electron donor yields:

$$\lambda_i(D) = \left(E_S(R_P) - E_S(R_S)\right) + \left(E_P(R_S) - E_P(R_P)\right) \quad \text{(Eq. 4)}$$

An analogous equation can be written for the electron acceptor. In the above equation, $E_s(R_p)$ is the energy of the species with the starting electron configuration and the product geometry; $E_s(R_s)$ is the energy of the optimised starting species; $E_p(R_s)$ is the energy of the species with the product electron configuration and the starting geometry and $E_p(R_p)$ is the energy of the optimised product species.

For calculations where electron transfer complexes are used, (Eq. 3) there is only one set of energies (where previously there were independent energies for the respective donor and acceptor molecules) thus affording (Eq. 5) simply as:

$$\lambda_i = \lambda_i(DA) \quad \text{(Eq. 5)}$$

where $\lambda_i(DA)$ is calculated in the same way as $\lambda_i(D)$. However, in these calculations, the reactant complex has singlet multiplicity while the product complex is calculated as a triplet; and there is no net change in the overall charge of the system.

Computational Details

Density Functional Theory (DFT) calculations were performed using the Gaussian 09 software package.[35] All reaction species were optimised using the M06-2X functional[36] with a double-zeta basis set. With the exception of potassium and iodine, all elements were modelled using the aug-cc-pVDZ basis set.[37] Potassium was modelled using the 6-31++G(d,p) basis set.[38] For systems that included iodine, the small-core energy consistent relativistic pseudopotential was implemented.[39, 40] Implicit solvation was modelled using the Conductor-like Polarizable Continuum Model (CPCM) with the associated parameters of benzene as the solvent. [41, 42 41, 4241, 42] Frequency calculations were performed on all optimised structures in order to characterise them as minima (zero imaginary frequencies) or maxima (single imaginary frequency). Gaussview 5.0.8 was used for structure visualisation.

Results and Discussion

Neutral Organic Super Electron Donors.

In order to establish baseline calculated activation energies, the first task was to reinvestigate the ability of the neutral organic SED's to reduce iodoarenes. For this part of the investigation, donors **21**-**23** were investigated using the two different reaction models. The first of these, Model 1, implements the standard Nelsen four-point method, where donor and acceptor molecules are independent of each other, to calculate the internal reorganisation energy. The second model, Model 2, uses a modified version of the Nelsen four-point method where the donor and acceptor are combined to form an electron transfer complex. This model determines the effect on the internal reorganisation energy of having a reaction partner in the system. For both of these models, 4-iodoanisole was chosen as the substrate.

The calculated electron transfer energetics for Model 1 (Table 1) show that the activation free energies (ΔG^*) for donors **21**-**23** would result in minimal conversion to the product under the reaction conditions (130 ^{o}C in a high-pressure reaction vessel for 3-5 hours). This is most evident for donor **21**, which has a calculated activation energy of 54.2 kcal/mol (Table 1). Donors **22** and **23** are also predicted to have high reaction barriers (40.2 and 39.5 kcal/mol respectively) using Model 1. Moreover, the highly endergonic nature of these reactions implies that even if the electron transfer occurs, the intermediate would be very short lived before collapsing to the reactant state despite the partial cleavage of the C—I bond. Therefore, electron transfer is considered to be extremely unfavourable under the Model 1. However, experimentally, **21** – **23** are efficient (super) electron donors.

Table 1. Comparison of activation and relative free energies [kcal/mol] calculated for neutral organic SED's **21**-**23**

Electron Donor	Electron Transfer Model			
	Model 1		Model 2	
	ΔG^*	ΔG_{rel}	ΔG^*	ΔG_{rel}
21	54.2	53.2	34.1	20.3
22	40.2	36.1	23.9	4.6
23	39.5	33.9	27.2	14.2

The results for Model 2 show that the use of an electron transfer complex produces a significant change in the electron transfer energetics. There is a decrease in the relative free energy of the electron transfer, such that, while still endergonic, the barrier to the reverse reaction is higher (13.0 – 19.3 kcal/mol, Table 1) thus making the reverse reaction more difficult relative to Model 1. Moreover, the use of the donor-acceptor complex in the calculation of the electron transfer energetics also results in a significant decrease in the calculated barrier heights by up to 19.3 kcal/mol (Table 1). For example, in the case of donor **22** as an example, the activation energy is decreased by 16.3 kcal/mol, and the relative free energy (ΔG_{rel}) is decreased by 31.5 kcal/mol, relative to Model 1, resulting in an electron transfer that is only mildly endergonic (ΔG_{rel} = 4.6 kcal/mol, Table 1). This suggests that the reorganisation of the electron transfer complex is more favourable than the reorganisation of the individual components.

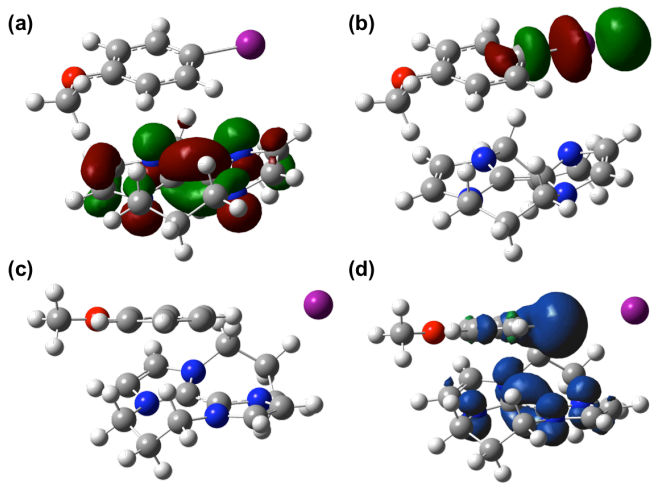

Figure 3. Calculated HOMO (a) and LUMO (b) for the reactant complex and the optimised geometry (c) and calculated spin density (d) for the product complex of donor **22**.

To ensure that the energetics calculated represent the transfer of an electron from the donor to the acceptor, rather than a singlet-to-triplet excitation localised on the electron donor, we probed the HOMO and LUMO of the reactant complex, as well as the spin density of the product complex, the visualisations of which are shown for donor **22** in Figure 3. Figure 3a shows that despite the formation of a stable complex, within the reactant complex the HOMO is localised predominantly on the donor molecule, while the Figure 3b shows that the LUMO is similarly localised on the acceptor. For the product complex (Figure 3c) the spin density of 2 is distributed relatively evenly across both the donor and acceptor components of the complex (Figure 3d). A decomposition of the atomic contributions to the spin densities shows that the 1.06 electrons is localised to the acceptor and 0.94 localised across the donor molecule (see Supporting Information Figures S1 and S3 for corresponding Figures of donors **21** and **23**).

Charged Organic Super Electron Donors

The charged organic SED's are proposed to form *in situ* from the reaction of a selection of simple organic molecules with potassium *tert*-butoxide. Figure 4 summarises the proposed SED's and the neutral precursors from which each is derived. The precursor selection includes compounds that are proven experimentally to lead to either efficient (blue in Figure 4) or inefficient (red in Figure 4) coupled product formation, and hence electron donor formation.

For these proposed donors, three reaction models will be addressed. Model 1, as with the previous section, will again consider the donor and acceptor molecules as separate entities. An alternative to Model 1 will include potassium counter ions (one counter ion for anionic systems, two counter ions for dianionic systems) to balance the charges of these donors, herein referred to as Model 1K. Finally, Model 2 will again represent the calculation of the electron transfer complex, and includes the potassium counter ions to give an overall neutral reaction system.

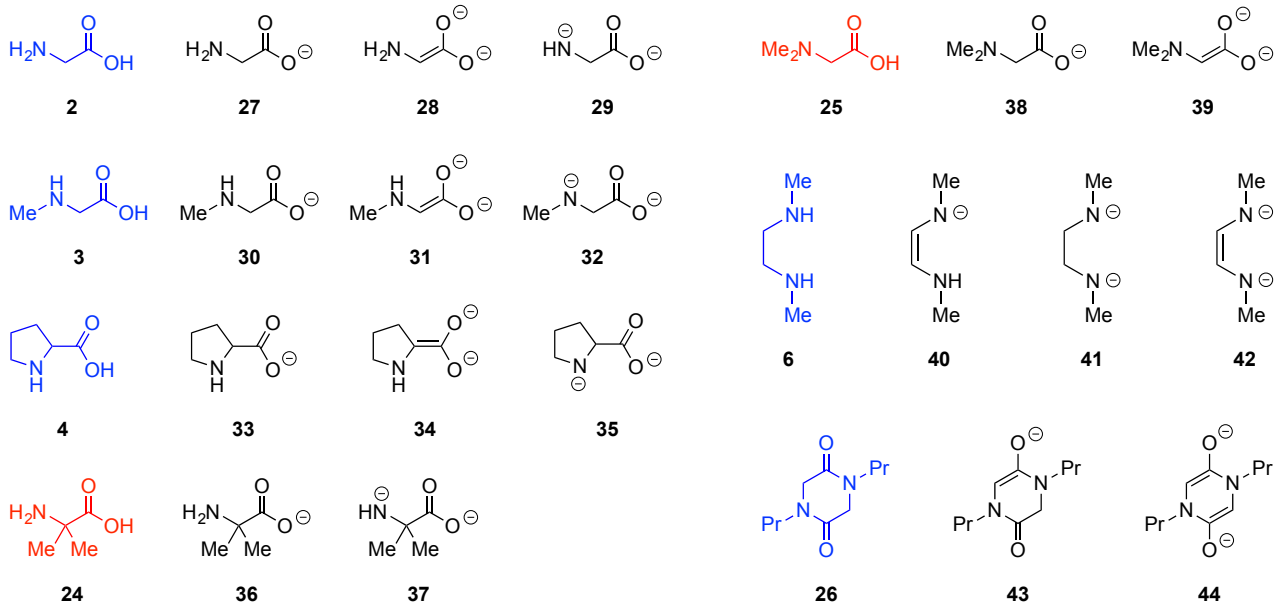

Figure 4. Precursors to proposed organic SED's are coloured blue to indicate precursors that are shown experimentally to result in efficient electron donors and red to indicate precursors that result in inefficient electron donors. The proposed structures of active organic SED's formed from the precursors upon reaction with potassium tert-butoxide are in black.

Calculation of Anionic Organic SED's. The initial deprotonation, by potassium *tert*-butoxide (KO^{t}Bu), of the precursor compounds **2**, **3**, **4**, **6**, **24**, **25** and **26**, results in a set of singly anionic species, which can act as electron donors. The calculated activation free energies for these potential donors using Model 1 show that the amino acid carboxylates **27**, **30**, **33**, **36**, and **38** are all predicted to be inefficient electron donors, with activation energies in excess of 49.0 kcal/mol (Table 2). These high activation energies and the instability of the resulting products (ΔG_{rel}, Table 2) are not consistent with

the experimentally observed efficiency of these donors. This suggests either a problem with the model calculations as observed for the neutral donors, or that the singly anionic species is not the active electron donor. In contrast, donors **40** and **43** are predicted to be efficient using this model, with activation energies of 18.3 and 26.2 kcal/mol respectively, and relatively stable product species.

The inclusion of the potassium counter ion in Model 1K for this series of candidate electron donors, raises the activation and relative free energies significantly. As in Model 1, the amino acid carboxylates are predicted to be inefficient donors, with activation energies, calculated using Model 1K, exceeding 85.0 kcal/mol (Table 2). More significantly however, donors **40** and **43** are now also predicted to be inefficient, with their respective activation energies for electron transfer now increased to 44.8 and 52.2 kcal/mol (Table 2). This increase across the board in the activation and relative free energies suggests that the simple inclusion of a counter ion to balance the charges in the systems is not beneficial in the calculation of the electron transfer energetics. Therefore, inclusion of the complete donor acceptor complex is required (Model 2) to ensure that the electron transfer energetics are modelled accurately.

Table 2. Summary of the activation and relative free energies [kcal/mol] calculated for anionic organic SED's.

Electron Donor	Model 1		Model 1K		Model 2	
	ΔG^*	ΔG_{rel}	ΔG^*	ΔG_{rel}	ΔG^*	ΔG_{rel}
27	53.6	43.4	99.5	99.2	64.7	58.3
30	50.3	38.7	92.0	91.6	64.9	58.8
33	49.6	43.5	89.7	89.6	65.7	59.5
36	51.5	39.8	95.0	94.9	64.3	58.3
38	49.9	44.1	85.8	88.6	65.1	58.9
40	15.3	-4.0	46.7	44.8	25.5	2.9
43	26.2	16.9	53.8	52.2	33.5	11.7

With Model 2, we note a significant decrease in the activation and relative free energies relative to Model 1K. However, relative to Model 1, the activation free energies are greater by approximately 10-16 kcal/mol. For the amino acid carboxylates, this results in activation free energies in the region of 64.0 kcal/mol, and as such are all considered inefficient donors. This suggests that the singly anionic state investigated is not the experimentally active form of the SED that results from these precursors. Interestingly, with donors **40** and **43**, we observe that the predicted activation free energies are once again accessible under the reaction conditions employed, at 25.5 and 33.5 kcal/mol, respectively. Moreover, the product state for **43** is further stabilised when the product state is treated as a complex, rather than the individual donor and acceptor molecules (Model 1, Table 2).

As with the neutral donors in the previous section, the reactant complex orbitals and product complex spin densities were investigated, and this yielded an unexpected result for the amino acid carboxylate complexes. A spin density of ~1 should exist on both the donor and acceptor molecules, in systems such as **30** (Figure 5a), which is observed (spin densities for the product complexes of all species investigated are available in the Supporting Information, Figures S4 – S21). However, the spin density on the acceptor molecule is localised onto the iodine atom, which is more typical of a homolytic bond scission of the neutral acceptor molecule rather than the radical anion that would result from electron transfer. This shows that within the singly anionic state these compounds are indeed not acting as electron donors. In contrast, donors **40** and **43**, display the expected spin density distribution across the donor and acceptor molecules, illustrated using **43** (Figure 5b).

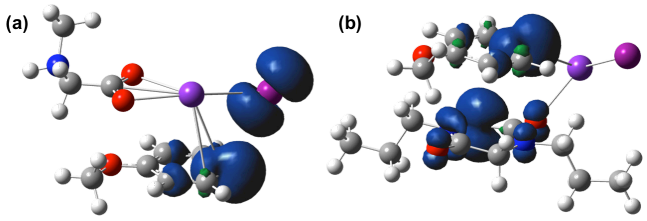

Figure 5. Spin densities calculated using Model 2 for donors **30** (a) and **43** (b).

Calculation of Dianionic Organic SED's. The calculated energetics for the amino acid carboxylates are not consistent with the experimentally observed activity of these compounds, therefore we propose that a dianionic species may be involved in the initiation of these transition metal-free coupling reactions. One notable exception to this proposal is when precursor **26** is used, as we have experimental precedent[23] to suggest that a monoanionic species such as **43** is sufficient to produce the desired reactivity, which is consistent with the calculated energetics presented in Table 2. Nonetheless, we consider the dianionic species **44**, resulting from a second deprotonation of **26** for completeness.

In the case of precursors **2**-**4**, there are two options for further deprotonation following the formation of the respective carboxylate anion; C—H deprotonation at the α-carbon (affording proposed donors **28**, **31** and **34**), or N—H deprotonation at the amine centre (affording proposed donors **29**, **32** and **35**). Structures **28**, **31** and **34** should represent stronger electron donors due to the formation of an electron-rich alkene, analogous to that observed in neutral organic SED's such as **22**. However, structures **29**, **32** and **35** could still represent active electron donors, despite the fact that the two negative charges in these structures are localised.

The two dimethylated variations of glycine, precursors **24** and **25**, can form only one dianionic species each (**37** and **39**), upon deprotonation of carboxylates **36** and **38**, owing to the substitution at the α-carbon and amine positions, respectively. For dianions **41** and **42**, the only difference is the presence of an alkene moiety linking the two anionic nitrogen centres, allowing the importance of this to be investigated. Dianion **44**, if formed *in situ*, is predicted to be a powerful electron donor due to its antiaromaticity. This antiaromaticity would be a very strong driving force for electron transfer, as loss of two electrons from this would afford an aromatic species, again

drawing similarity to the neutral organic SED's discussed previously.

The calculated energetics for these dianionic organic electron donors are summarised in Table 3. Using Model 1, it is predicted that all dianionic species represent very powerful electron donors, with the highest activation barrier calculated at a mere 2.7 kcal/mol. This in contrast to the experimental observation that using amino acids **24** and **25** as initiators in biaryl coupling reactions leads to poor yields. This observation implies that dianions **37** and **39**, if formed *in situ*, are inefficient electron donors. We believe that this disagreement between theory and experiment suggests that Model 1 is unable to provide a realistic representation of the electron transfer energetics for these highly charged species.

Table 3. Summary of the activation and relative free energies [kcal/mol] calculated for dianionic organic SED's.

Electron Donor	Model 1		Model 1K		Model 2	
	ΔG^*	ΔG_{rel}	ΔG^*	ΔG_{rel}	ΔG^*	ΔG_{rel}
28	0.2	-64.5	33.0	22.9	15.2	-14.9
29	1.8	-39.1	43.9	42.3	25.9	1.3
31	0.2	-62.3	35.7	28.3	19.1	-8.8
32	1.8	-41.7	38.9	35.7	25.4	-1.5
34	0.6	-60.2	31.5	23.2	11.3	-14.0
35	2.7	-39.7	40.0	36.5	25.5	-4.9
37	1.9	-40.8	43.2	41.4	30.5	3.9
39	0.7	-54.9	36.2	27.7	20.3	-8.0
41	2.0	-41.6	40.6	37.6	24.2	-6.0
42	0.3	-71.8	27.7	18.8	3.0	-25.6
44	1.1	-53.6	31.6	18.5	15.0	-11.8

Using Model 1K, some differences become more obvious in the comparison of potential donors formed from amino acids (precursors **2**, **3**, **4**, **24** and **25**). With this model, it is apparent that dianions **28**, **31**, **34** and **39** are all predicted to have activation energies approximately 3-10 kcal/mol lower than donors **29**, **32**, **35** and **37** respectively. This offers support for the proposal that the dianions formed from C—H deprotonation do afford electron donors stronger than those formed from N—H deprotonation of amino acid carboxylates. In the case of the proposed donors **41** and **42**, both derived from precursor **6**, there is a difference in activation energy of approximately 13.0 kcal/mol when the alkene moiety is included in Model 1K. Similar to the amino acid subset, this shows that it is clearly important to have an electron-rich alkene present to delocalise the negative charges. For donor **44**, Model 1K predicts an activation energy of 31.6 kcal/mol, which is achievable under the reaction conditions used.

The use of the donor-acceptor complexes (Model 2) for these systems leads to a significant decrease in both the activation and relative free energies for all the proposed donors relative to Model 1K. As was observed for the monoanionic donors, despite the decrease relative to Model 1K, these energies are greater than those obtained using Model 1. For donors **28**, **31**, **34** and **39** the activation free energies decrease by approximately 16.0 kcal/mol each compared to Model 1K, making all four easily accessible under the reaction conditions. The activation free energies for the corresponding dianions formed by N—H deprotonation (donors **29**, **32**, **35** and **37**) also decrease by approximately 13.0 kcal/mol moving from Model 1K to Model 2, again bringing these candidates below the upper limit of activation. Comparing these two subsets, we note that Model 2 maintains the trend that dianions formed from C—H deprotonation of amino acid carboxylates afford more effective electron donors than those formed from N—H deprotonation. This is evidenced by both a lower activation and relative free energy for donors **28**, **31**, **34** and **39**. The two dianions formed from precursor **6** (**41** and **42**) demonstrate the same trend as was observed using Model 1K, in that the presence of the alkene moiety leads to a more effective electron donor (their respective activation energies amounting to 24.2 and 3.0 kcal/mol). For dianion **44**, derived from a double deprotonation of **26**, an accessible activation free energy of 15.0 kcal/mol is predicted using Model 2.

With the energetics for the reduction of an aryl iodide by the charged donors **27**-**44** established, it is clear that the differences in activation energy for the electron transfer from donors derived from both effective and ineffective precursors (based on experimental observation) are not always sufficient to account for the observed difference in activity. For example, using precursor **3** as an additive leads to efficient coupling, while the use of **25** does not. The results from Marcus Hush theory using Model 2 indicate a difference in activation free energy of only 1.2 kcal/mol between dianions **31** and **39**, indicating that the electron transfer reaction is not the limiting step in these reactions. Therefore, the formation of the active species must be the limiting step for the inactive compounds.

Formation of Charged Organic SED's

Given the predicted reactivities of the structures bearing an electron-rich alkene group, we chose to focus our investigation on the formation of these candidates. In probing these pathways, the transition states for the deprotonation of carboxylic acid groups for the amino acid additives (**2**, **3**, **4**, **24** and **25)** could not be located, nor could the reactant complex, suggesting a barrierless forward process. The resulting carboxylate was therefore taken as the starting point for the subsequent deprotonations. Similarly, for the N—H deprotonation of amino acids (**30** → **32**), it was found that the reverse reaction proceeded in a barrierless manner, resulting in the exclusive formation of the reactant complex. The proposed pathways towards the donors studied in this work are summarised in Scheme 4.

Looking at the energetics for the formation of dianions **28**, **31**, **34** and **39** (Table 4) it is noted that these reactions are disfavoured when we consider the free energy, with the reverse reaction being strongly favoured. In order to illustrate that the calculated structures represent true maxima and minima, the electronic energies are also provided, which show the relative energy to be lower than the activation energy. Interestingly, for the deprotonation leading to **39**, we note that there is an approximate 10.0 kcal/mol increase in the

activation energy relative to the remaining amino acid dianions (entries 1-3), likely to be a consequence of the additional allylic strain imparted on the molecule in forming the enolate.

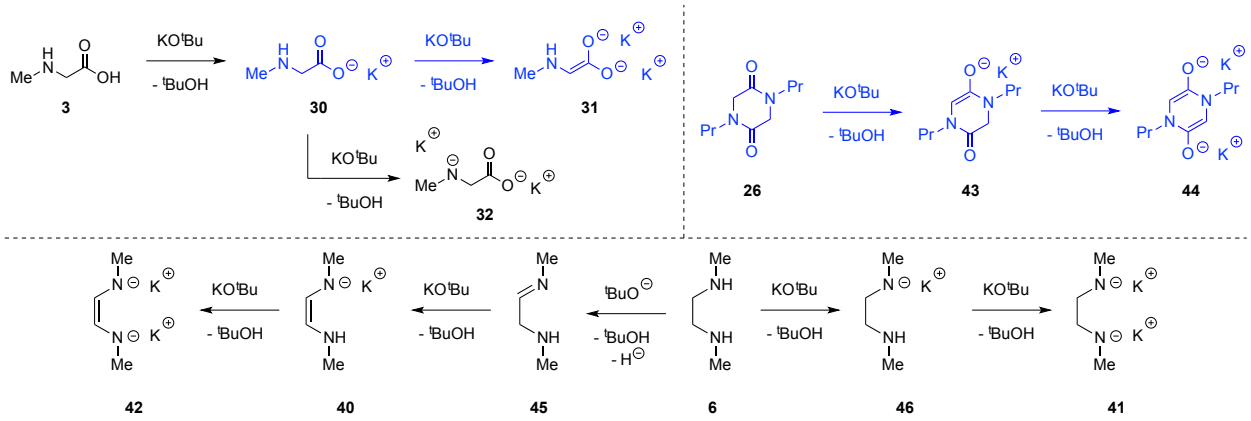

Scheme 4. Summary of proposed pathways towards the donor candidates investigated in this work. Reactions in blue indicate pathways that were modelled in detail.

Table 4. Summary of the activation and relative free energies and electronic energies [kcal/mol] calculated for the formation of selected charged organic SED's.

Deprotonation Reaction Step	Gibbs Free Energy		Electronic Energy	
	ΔG^*	ΔG_{rel}	ΔE^*	ΔE_{rel}
27 → 28	14.7	16.2	17.1	16.2
30 → 31	13.6	15.7	16.1	15.1
33 → 34	14.3	15.4	15.2	14.4
38 → 39	24.4	23.2	26.7	25.6
26 → 43	3.6	0.23	5.5	-0.1
43 → 44	12.4	12.6	13.7	12.7

The instability of the dianions resulting from these deprotonations suggests that for an electron transfer to occur the true activation energy for the electron transfer should include the energy required to reach the dianion, as it will have a limited lifetime once formed. For example, the electron transfer from **31** requires the formation of **31** from **30** in an endergonic reaction of 15.7 kcal/mol (Table 4), with the subsequent electron transfer requiring an activation energy of 19.1 kcal/mol (Table 3). Therefore, for **3** to act as an electron donor, the initial exothermic reaction to form **30** takes place in a barrierless reaction, which then requires 34.8 kcal/mol to form the electron donor **31** and the immediate transfer of the electron to the iodobenzene acceptor. If the acceptor is not present then **31** will collapse back to **30** without the transfer of an electron. Nonetheless, the overall barrier for electron transfer of 34.8 kcal/mol is still achievable under the reaction conditions, which require the reaction to be performed at 120 ºC. A similar analysis applies to donors **28** and **34**, which have comparable energetics to **31**.

In contrast, for **39**, the initial formation of **38** also occurs in a barrierless reaction. However, the increased endergonicity for the formation of **39** (23.2 kcal/mol, Table 4) results in a significantly larger overall barrier for the electron transfer from **39** of 43.5 kcal/mol (23.2 kcal/mol for formation of **39** and 20.3 kcal/mol for the electron transfer, Table 3). This higher activation energy for the electron transfer is not accessible under the reaction conditions.

For the two deprotonations of precursor **26** (entries 5 and 6), we note two accessible barriers for the first and second deprotonations (3.6 and 12.4 kcal/mol respectively). For the deprotonation leading to **44** (entry 6), the electronic energy values again demonstrate that the structures correctly represent a reaction maximum and two reaction minima.

Conclusions

Based on the outcomes of this study, the prediction of candidate electron donors is reliant on both the electron transfer energetics as calculated using Marcus Hush theory and, in the case of charged electron donors, the energetics for their formation. For all of the donors investigated, Model 2 represents a more reliable method for calculating electron transfer energetics. The calculated activation and relative free energies using Model 2 were consistently more favourable than those calculated using Model 1K. Model 1 represents an overestimation of activation free energies for neutral donors **21**-**23**. For these donors, using Model 2 rather than Model 1 produces a $\Delta\Delta G^*$ of between 11.3-19.3 kcal/mol. Additionally, Model 1 underestimates the activation free energies for dianionic electron donors compared to Model 2, as there is minimal discrepancy between, for example, donors **31** and **32** ($\Delta\Delta G^*$ = 1.6 kcal/mol using Model 1; 6.3 kcal/mol using Model 2).

Candidates that are predisposed to form an electron-rich alkene upon reaction with a strong base, such as that found in donors **31**, **42** and **43**, are able to produce efficient electron donors. The exceptions to this proposition are instances where the precursor has significant substitution on any of the groups α– to where the alkene would be formed, such as in the formation of donor **39** which has an overall barrier to electron transfer of 43.5 kcal/mol.

Acknowledgements

We would like to thank the EPSRC (grant no. EP/K033077/1) and GlaxoSmithKline for funding. Results were obtained using the EPSRC funded ARCHIE-WeSt High Performance Computer (www.archie-west.ac.uk). EPSRC grant no. EP/K000586/1.

References

1. M. R. Wasielewski, *Chem. Rev.*, 1992, **92**, 435-461.
2. H. Lodish, A. Berk, P. Matsudaira, C. A. Kaiser, M. Krieger, M. P. Scott, L. Zipursky and J. Darnell, in *Molecular Cell Biology, 5th Edition*, W. H. Freeman, New York, 2003, ch. 8, Cellular Energetics.
3. A. J. Birch, *J. Chem. Soc.*, 1944, DOI: 10.1039/JR9440000430, 430-436.
4. Y. Lin, Y. Li and X. Zhan, *Chem. Soc. Rev.*, 2012, **41**, 4245-4272.
5. C. K. Prier, D. A. Rankic and D. W. C. MacMillan, *Chem. Rev.*, 2013, **113**, 5322-5363.
6. C.-L. Sun and Z.-J. Shi, *Chem. Rev.*, 2014, **114**, 9219-9280.
7. D. P. Hari and B. Koenig, *Angew. Chem. Int. Ed.*, 2013, **52**, 4734-4743.
8. I. Ghosh, T. Ghosh, J. I. Bardagi and B. König, *Science*, 2014, **346**, 725-728.
9. C. L. Sun, H. Li, D. G. Yu, M. Yu, X. Zhou, X. Y. Lu, K. Huang, S. F. Zheng, B. J. Li and Z. J. Shi, *Nat. Chem.*, 2010, **2**, 1044-1049.
10. K. Tanimoro, M. Ueno, K. Takeda, M. Kirihata and S. Tanimori, *J. Org. Chem.*, 2012, **77**, 7844-7849.
11. W. Liu, H. Cao, H. Zhang, H. Zhang, K. H. Chung, C. He, H. Wang, F. Y. Kwong and A. Lei, *J. Am. Chem. Soc.*, 2010, **132**, 16737-16740.
12. W. Liu, F. Tian, X. Wang, H. Yu and Y. Bi, *Chem. Commun.*, 2013, **49**, 2983-2985.
13. Y. S. Ng, C. S. Chan and K. S. Chan, *Tetrahedron Lett.*, 2012, **53**, 3911-3914.
14. C. L. Sun, Y. F. Gu, B. Wang and Z. J. Shi, *Chem. -Eur. J.*, 2011, **17**, 10844-10847.
15. S. Sharma, M. Kumar, V. Kumar and N. Kumar, *Tetrahedron Lett.*, 2013, **54**, 4868-4871.
16. Y. Wu, P. Y. Choy and F. Y. Kwong, *Org. Biomol. Chem.*, 2014, **12**, 6820-6823.
17. Y. Wu, S. M. Wong, F. Mao, T. L. Chan and F. Y. Kwong, *Org. Lett.*, 2012, **14**, 5306-5309.
18. Y. Qiu, Y. Liu, K. Yang, W. Hong, Z. Li, Z. Wang, Z. Yao and S. Jiang, *Org. Lett.*, 2011, **13**, 3556-3559.
19. S. Yanagisawa, K. Ueda, T. Taniguchi and K. Itami, *Org. Lett.*, 2008, **10**, 4673-4676.
20. A. Studer and D. P. Curran, *Angew. Chem. Int. Ed.*, 2011, **50**, 5018-5022.
21. J. A. Murphy, *J. Org. Chem.*, 2014, **79**, 3731-3746.
22. S. Zhou, G. M. Anderson, B. Mondal, E. Doni, V. Ironmonger, M. Kranz, T. Tuttle and J. A. Murphy, *Chem. Sci.*, 2014, **5**, 476-482.
23. S. Zhou, E. Doni, G. M. Anderson, R. G. Kane, S. W. MacDougall, V. M. Ironmonger, T. Tuttle and J. A. Murphy, *J. Am. Chem. Soc.*, 2014, **136**, 17818-17826.
24. J. A. Murphy, T. A. Khan, S. Z. Zhou, D. W. Thomson and M. Mahesh, *Angew. Chem. Int. Ed.*, 2005, **44**, 1356-1360.
25. S. S. Hanson, E. Doni, K. T. Traboulsee, G. Coulthard, J. A. Murphy and C. A. Dyker, *Angew. Chem. Int. Ed.*, 2015, **54**, 11236-11239.
26. S. V. Rosokha, J.-M. Lü, M. D. Newton and J. K. Kochi, *J. Am. Chem. Soc.*, 2005, **127**, 7411-7420.
27. S. V. Rosokha, M. D. Newton, M. Head-Gordon and J. K. Kochi, *Chem. Phys.*, 2006, **324**, 117-128.
28. S. V. Rosokha, S. M. Dibrov, T. Y. Rosokha and J. K. Kochi, *Photochem. Photobiol. Sci.*, 2006, **5**, 914-924.
29. S. Kazemiabnavi, P. Dutta and S. Banerjee, *J. Phys. Chem. C.*, 2014, **118**, 27183-27192.
30. J. Blumberger, *Phys. Chem. Chem. Phys.*, 2008, **10**, 5651-5667.
31. J. A. Murphy, S.-z. Zhou, D. W. Thomson, F. Schoenebeck, M. Mahesh, S. R. Park, T. Tuttle and L. E. A. Berlouis, *Angew. Chem. Int. Ed.*, 2007, **46**, 5178-5183.
32. S. F. Nelsen, S. C. Blackstock and Y. Kim, *J. Am. Chem. Soc.*, 1987, **109**, 677-682.
33. B. Eberle, O. Hübner, A. Ziesak, E. Kaifer and H.-J. Himmel, *Chem. Eur. J.*, 2015, **21**, 8578-8590.
34. R. A. Marcus, *J. Chem. Phys.*, 1965, **43**, 679-701.
35. Gaussian 09, Revision D.01, M. J. Frisch, G. W. Trucks, H. B. Schlegel, G. E. Scuseria, M. A. Robb, J. R. Cheeseman, G. Scalmani, V. Barone, B. Mennucci, G. A. Petersson, H. Nakatsuji, M. Caricato, X. Li, H. P. Hratchian, A. F. Izmaylov, J. Bloino, G. Zheng, J. L. Sonnenberg, M. Hada, M. Ehara, K. Toyota, R. Fukuda, J. Hasegawa, M. Ishida, T. Nakajima, Y. Honda, O. Kitao, H. Nakai, T. Vreven, J. A. Montgomery Jr., J. E. Peralta, F. Ogliaro, M. J. Bearpark, J. Heyd, E. N. Brothers, K. N. Kudin, V. N. Staroverov, R. Kobayashi, J. Normand, K. Raghavachari, A. P. Rendell, J. C. Burant, S. S. Iyengar, J. Tomasi, M. Cossi, N. Rega, N. J. Millam, M. Klene, J. E. Knox, J. B. Cross, V. Bakken, C. Adamo, J. Jaramillo, R. Gomperts, R. E. Stratmann, O. Yazyev, A. J. Austin, R. Cammi, C. Pomelli, J. W. Ochterski, R. L. Martin, K. Morokuma, V. G. Zakrzewski, G. A. Voth, P. Salvador, J. J. Dannenberg, S. Dapprich, A. D. Daniels, Ö. Farkas, J. B. Foresman, J. V. Ortiz, J. Cioslowski and D. J. Fox, Gaussian, Inc., Wallingford, CT, USA, 2009
36. Y. Zhao and D. G. Truhlar, *Acc. Chem. Res.*, 2008, **41**, 157-167.
37. T. H. Dunning, *J. Chem. Phys.*, 1989, **90**, 1007-1023.
38. V. A. Rassolov, M. A. Ratner, J. A. Pople, P. C. Redfern and L. A. Curtiss, *J. Comput. Chem*, 2001, **22**, 976-984.
39. K. A. Peterson, D. Figgen, E. Goll, H. Stoll and M. Dolg, *J. Chem. Phys.*, 2003, **119**, 11113-11123.
40. K. A. Peterson, B. C. Shepler, D. Figgen and H. Stoll, *J. Phys. Chem. A.*, 2006, **110**, 13877-13883.
41. V. Barone and M. Cossi, *J. Phys. Chem. A.*, 1998, **102**, 1995-2001.
42. M. Cossi, N. Rega, G. Scalmani and V. Barone, *J. Comput. Chem.*, 2003, **24**, 669-681.